Site-specific Orientation of an α-helical Peptide Ovispirin-1 from Isotope Labeled SFG Spectroscopy

Bei Ding, Jennifer E. Laaser, Yuwei Liu, Pengrui Wang, Martin T. Zanni, Zhan Chen**

Department of Chemistry, University of Michigan, Ann Arbor, MI 48109

[2]Department of Chemistry, University of Wisconsin-Madison, Madison, WI 53703

August 2013

*To whom all correspondence should be addressed

Email: zhanc@umich.edu, Fax: 734-647-4685; zanni@chem.wisc.edu, Fax: 608-262-9918

1. SFG data analysis

The intensity of SFG signal is proportional to the square of the effective second-order nonlinear optical susceptibility. [1]

$$\chi_{\mathrm{eff}}^{(2)} = \chi_{\mathrm{nr}}^{(2)} + \sum_q \frac{A_q}{\omega_n - \omega_q + i\Gamma_q} \qquad \text{(s1)}$$

where χ_{nr} is the nonresonant signal, A_q is the signal strength, ω_n and ω_q represent the tunable infrared beam frequency and the peak center for a particular mode, and Γ_q is the damping coefficient.

In the SFG experiment, we collected SFG signals using different polarization combinations of the input and output laser beams including ssp and ppp. The effective second order nonlinear optical susceptibility components $\chi_{\mathrm{eff,ssp}}^{(2)}$ and $\chi_{\mathrm{eff,ppp}}^{(2)}$ which we can measure in the experiments can be related to the components of the susceptibility defined in the lab-frame coordinates $\chi_{\mathrm{xxz}}^{(2)}$ and $\chi_{\mathrm{zzz}}^{(2)}$ through the Fresnel coefficients:

$$\chi_{\mathrm{eff,ssp}}^{(2)} = \mathrm{L_{xxz}}\chi_{\mathrm{xxz}}^{(2)} \qquad \text{(s2)}$$

$$\chi_{\mathrm{eff,ppp}}^{(2)} = \mathrm{L_{xxz}}\chi_{\mathrm{xxz}}^{(2)} + \mathrm{L_{xzx}}\chi_{\mathrm{xzx}}^{(2)} + \mathrm{L_{zxx}}\chi_{\mathrm{zxx}}^{(2)} + \mathrm{L_{zzz}}\chi_{\mathrm{zzz}}^{(2)} \qquad \text{(s3)}$$

The ratio $\chi_{\mathrm{xxz}}^{(2)}/\chi_{\mathrm{zzz}}^{(2)}$ discussed in the paper can be calculated from the fitting parameters of the experimental spectra or $\chi_{\mathrm{eff,ssp}}^{(2)}/\chi_{\mathrm{eff,ppp}}^{(2)}$.

2. Calculation Details of Hamiltonian approach

a – Definition of the molecular response for a single amide-I unit

The molecular axes for an individual amide-I unit are defined such that the C(O)N bond lies in the bc-plane (molecular yz plane), with the CO bond tilted 34 degrees from the c axis, as shown in Fig. S1.

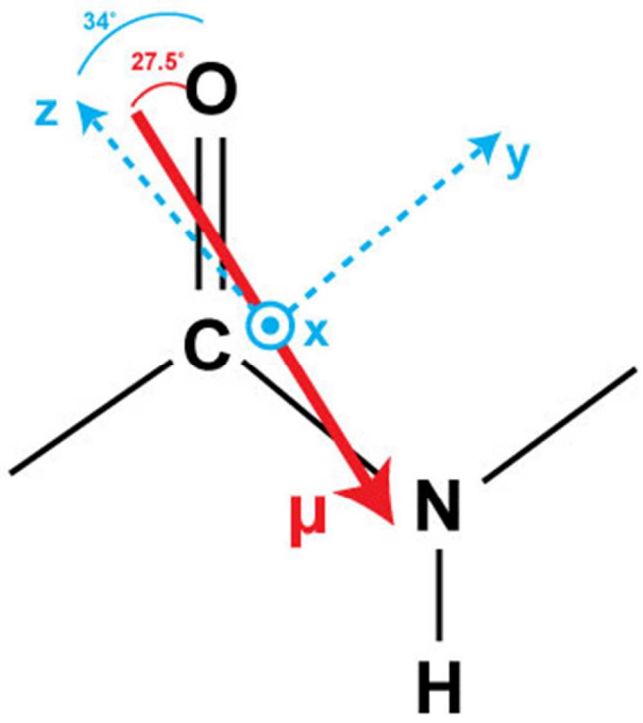

Figure S1. Diagram illustrating the orientation of the molecular response with respect to the amide-I bond. The red arrow indicates the direction and effective location of the transition dipole; the blue axes indicate the principle axes of the Raman polarizability.

In this frame, the transition dipole is defined as

$$\mu = \begin{pmatrix} 0 \\ -\sin\frac{6.5\pi}{180} \\ -\cos\frac{6.5\pi}{180} \end{pmatrix}$$

such that it is oriented 27.5 degrees from the CO bond. This angle was chosen to ensure that the angle of a single amide-I transition dipole relative to the axis of an ideal alpha helix was 42 degrees (see below), consistent with prior calculations.

The molecular-frame transition polarizability is defined as

$$\alpha = \begin{pmatrix} 0.25 & 0 & 0 \\ 0 & 1 & 0 \\ 0 & 0 & 5 \end{pmatrix}$$

as reported[2]. Thus the chromophore is most polarizable along the molecular c-axis, 34 degrees from the CO bond, and least polarizable along the molecular a-axis, out of the plane of the C(O)N bond.

The "center", or effective position, of the vibrational mode is defined to be

$$\vec{r}_{amide-I} = \vec{r}_C + 0.665\hat{r}_{CO} + 0.256\hat{r}_{CN}$$

where $\vec{r}_C$ is the position of the carbon atom, $\hat{r}_{CO}$ is the unit vector along the CO bond, and $\hat{r}_{CN}$ is the unit vector along the CN bond, with all positions given in Angstroms[3]. This position is used to calculate the distance between coupled modes, as necessary for the transition dipole coupling calculations as described below.

b – Transition dipole coupling and normal mode calculations

For each C(O)N bond in the peptide structure, the single-residue response defined above was rotated and translated into the helix (or peptide) molecular frame, as described previously[4]. For the ideal helix structure, with the helix axis oriented along the z-axis and the transition dipole of the first mode lying in the xz plane, the single-residue response in the helix frame was

$$\mu = \begin{pmatrix} 0.67 \\ 0 \\ 0.74 \end{pmatrix}$$

corresponding to a transition dipole tilted 42 degrees from the helix axis, and

$$\alpha = \begin{pmatrix} 0.64 & 0.03 & 0.40 \\ 0.03 & 0.06 & -0.01 \\ .40 & -0.01 & 0.55 \end{pmatrix}$$

which corresponds closely to previous reports[2].

Once each local mode was rotated into the peptide frame, their couplings were calculated using the transition dipole coupling model,

$$\beta_{ij} = \frac{1}{4\pi\epsilon_0}\left[\frac{\vec{\mu}_i \cdot \vec{\mu}_j}{r_{ij}^3} - 3\frac{(\vec{r}_{ij} \cdot \vec{\mu}_i)(\vec{r}_{ij} \cdot \vec{\mu}_j)}{r_{ij}^5}\right]$$

where β_{ij} is the coupling between modes i and j, the $\vec{\mu}$'s are the transition dipoles of the two modes, and $\vec{r}_{ij}$ is the vector connecting the center position of the two modes. Coupling values for $|i-j| = 1$ were multiplied by a factor of 0.73 to give better agreement with typical coupling constants for alpha helices[3].

The Hamiltonian was then constructed in the local mode system, using the calculated couplings for the off-diagonal elements and the local mode frequencies for the on-diagonal elements. We used a local mode frequency of 1645 cm^{-1} for unlabeled ($^{12}C=^{16}O$). For the labeled mode, we used a frequency of 1600 cm^{-1}. This frequency is slightly lower than the 1608 cm^{-1} frequency observed in the experimental spectra, but the larger frequency separation was necessary to easily distinguish the labeled peak from the unlabeled peak in the ensuing calculations, and did not seem to significantly affect our analysis.

The Hamiltonian was diagonalized, and the normal mode transition dipoles were calculated using

$$\mu_N = \sum_m C_{Nm}\mu_m$$

where $\mu_m$is the local mode transition dipole, μ_N is the normal mode transition dipole, and C_{Nm} is the element of the eigenvector giving the contribution of local mode m to normal mode N. The normal mode Raman tensors were calculated using an analogous formula (replace μ with α).

The normal mode hyperpolarizabilities β were then calculated by taking the outer product of μ and α:

$$\beta = \alpha \otimes \mu$$

The normal mode hyperpolarizabilities were then rotated into the lab frame to calculate the lab-frame responses χ, as has been described previously[4].

To calculate simulated spectra, we summed a series of Lorentzians centered at the normal mode frequencies and multiplied by the mode's χ value. To calculate the total χ value for the labeled peak, we summed over all normal modes with frequencies less than 1610 cm^{-1}. The unlabeled peak χ values were correspondingly determined by summing over all normal modes with frequencies >= 1610 cm^{-1}. A more accurate method would be to fit the simulated spectra to a pair of peaks, but applying a simple cutoff was computationally much faster and did not yield significantly different results.

3. SFG spectra of isotope labeled ovispirin-1 associated with the lipid bilayer

The dipalmitoylphosphatidyglycerol (DPPG)/deuterated dipalmitoylphosphatidyglycerol (dDPPG) lipid bilayer system was constructed with the Langmuir-Blodgett method as previously reported[5]. A KSV2000 LB system was used to deposit the first DPPG (mono) layer on one of the square faces of a right-angle prism. Then 2 mL reservoir was placed on the sample stage of the SFG system right below the spot where the two laser beams overlap. After finding the monolayer signal, we spread a certain amount of deuterated DPPG lipid on the water surface in the reservoir to reach a surface pressure of 34 mN/m. The reservoir was then lifted to contact with the lipid monolayer deposited on the CaF_2 surface to form a lipid bilayer. 40 μL ovispirin-1 stock peptide solution (0.5mg/mL) in 10mM pH=7.1 phosphate buffer was added to the water subphase (in the

reservoir, ~2000 mL). The final peptide concentration was 10 μg/mL. SFG amide I signal from the peptide reached equilibrium after ~20 min and remained stable for the next 2 hrs. The peak at ~1655 cm^{-1} is typical for α-helical signal (Figure s1). The small peak at ~1725 cm^{-1} is from the lipid carbonyl group (Figure s1). The peakwidth is ~17.5 cm^{-1} for G4 and ~19.0 cm^{-1} for G8 isotope label peak.

(a)

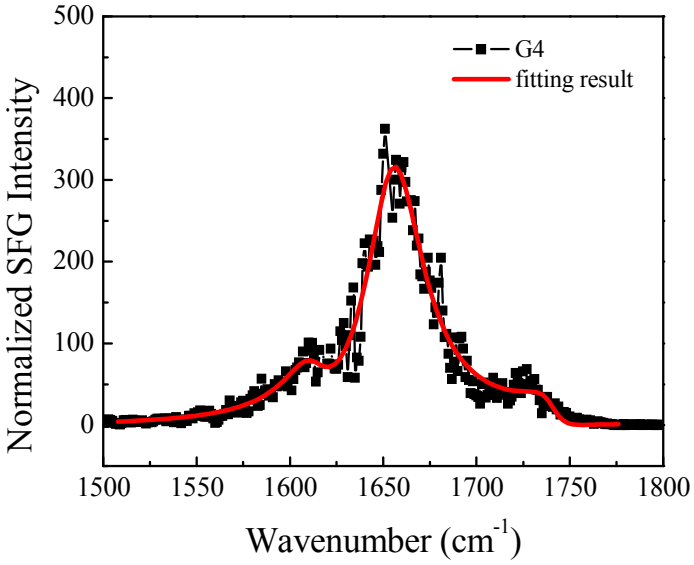

(b)

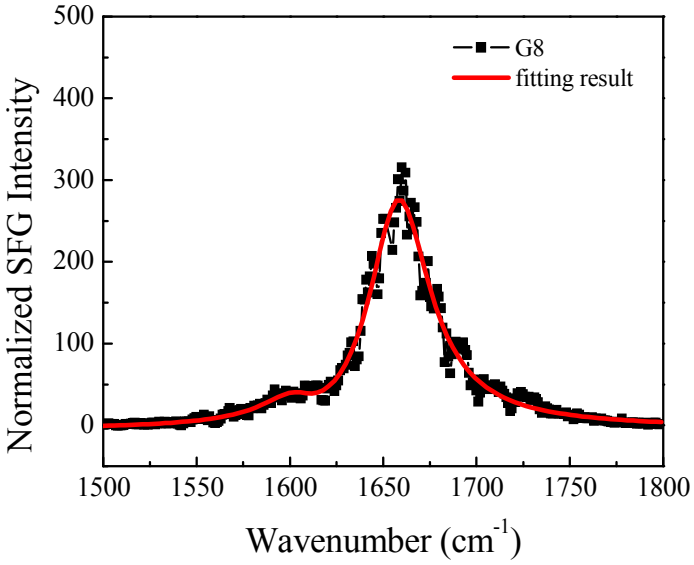

Figure s1: SFG ppp spectra of ovispirin-1 mutated at a) site 4 and b) site 8 with $^{13}C=^{16}O$ glycine.

4. SFG amide I signals dominated by the contribution from the α-helical structure

The previous NMR study suggested that the α-helical structure in ovispirin-1 spans from residue 4 to residue 16 among all 18 residues. To investigate the contribution from the α-helical region to the observed SFG amide I, we used NLOPredict[6] to quantitively assess the percentage of the helical and random coil contribution (Figure s2). Figure s2 suggests that, when deducing the orientation by the SFG amide I signals, it is reasonable to assume that nearly all the signals are from the α-helical component.

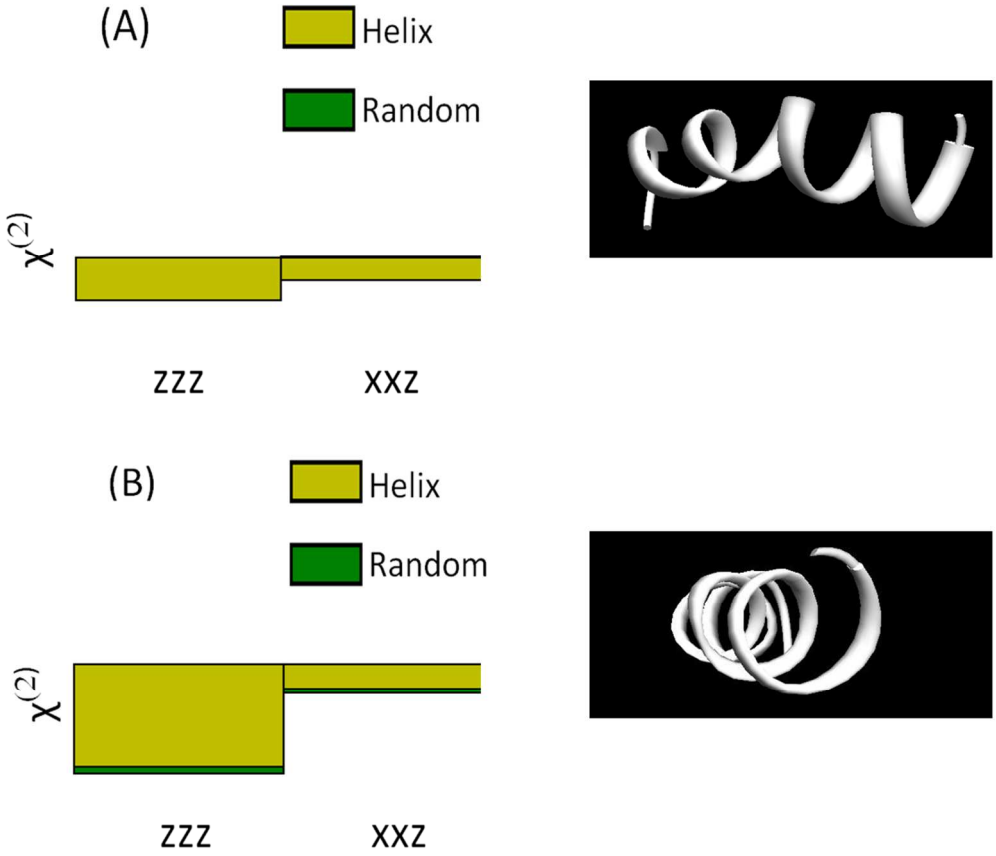

Figure s2: The contributions to the macroscopic SFG $\chi^{(2)}$ zzz and xxz components calculated by NLOPredict. The lipid bilayer surface is considered to be parallel to the surface of the paper. (A)

The ovispirin-1 molecule is nearly lying down on the surface; (B) Ovispirin-1 adopts a nearly perpendicular orientation on the polymer surface. For both cases, the contributions from the random coiled structure are minimal (<10%).

References

(1) Wang, J.; Lee, S.-H.; Chen, Z. *J. Phys. Chem. B*. **2008**, *112*, 2281-2290.

(2) Nguyen, K. T.; Clair, S. V. Le; Ye, S.; Chen, Z. *J. Phys. Chem. B*. **2009**, *113*, 12169-12180.

(3) Hamm, P.; Zanni, M. *Concepts and Methods of 2D Infrared Spectroscopy*; Cambridge University Press: Cambridge, U.K., 2011.

(4) Laaser, J. E.; Zanni, M. T. *J. Phys. Chem. A*. **2013**, Article ASAP

(5) Ye, S.; Nguyen, K. T.; Le Clair, S. V.; Chen, Z., *J. Struct. Biol.* **2009**, 168, 61-77.

(6) Moad, A. J.; Moad, C. W.; Perry, J. M.; Wampler, R. D.; Goeken, G. S.; Begue, N. J.; Shen, T.; Heiland, R.; Simpson, G. J. *J. Comp. Chem.* **2007**, *28*, 1996-2002.